Optical Polarization Möbius Strips and Points of Purely Transverse Spin Density

Thomas Bauer,[1,2] Martin Neugebauer,[1,2] Gerd Leuchs,[1,2,3] and Peter Banzer[1,2,3,*]
[1]Max Planck Institute for the Science of Light, Guenther-Scharowsky-Straße 1, D-91058 Erlangen, Germany
[2]Institute of Optics, Information and Photonics, University Erlangen-Nuremberg, Staudtstraße 7/B2, D-91058 Erlangen, Germany
[3]Department of Physics, University of Ottawa, 25 Templeton, Ottawa, Ontario K1N 6N5, Canada
(Received 4 March 2016; published 28 June 2016)

Tightly focused light beams can exhibit complex and versatile structured electric field distributions. The local field may spin around any axis including a transverse axis perpendicular to the beams' propagation direction. At certain focal positions, the corresponding local polarization ellipse can even degenerate into a perfect circle, representing a point of circular polarization or *C* point. We consider the most fundamental case of a linearly polarized Gaussian beam, where—upon tight focusing—those *C* points created by transversely spinning fields can form the center of 3D optical polarization topologies when choosing the plane of observation appropriately. Because of the high symmetry of the focal field, these polarization topologies exhibit nontrivial structures similar to Möbius strips. We use a direct physical measure to find *C* points with an arbitrarily oriented spinning axis of the electric field and experimentally investigate the fully three-dimensional polarization topologies surrounding these *C* points by exploiting an amplitude and phase reconstruction technique.

DOI: 10.1103/PhysRevLett.117.013601

Introduction.—Structured light fields represent important tools in modern optics due to their multitude of different applications, for example, in microscopy [1–3], nano-optics [4–7], and optical trapping [8,9]. In general, the spatial tailoring of the amplitude, phase, and polarization of paraxial or nonparaxial light beams can lead to interesting topological structures of the electric field such as phase vortices [10,11], optical knots [12,13], and optical polarization Möbius strips [14–17]. The latter are linked to the presence of so-called *C* points or *C* lines in the field distribution, i.e., positions where the local polarization ellipse degenerates to a circle and the field is thus circularly polarized [18]. While polarization Möbius strips have been predicted a decade ago and investigated ever since [19], only recent advances in nano-optics, in particular, 3D amplitude and phase reconstruction techniques at the nanoscale [20], have enabled their experimental verification [16]. This was achieved by tightly focusing a light beam with spatially varying polarization spanning the full Poincaré sphere [21–23]. In the focal plane of such a full Poincaré beam, this yields a complex fully vectorial field structure, including a *C* point on the optical axis with the electric field spinning around said (longitudinal) axis. Tracing the major axis of the polarization ellipse around this *C* point allowed for revealing optical polarization Möbius strips hidden in the focal polarization distribution [16].

In more general field distributions, *C* points with an arbitrarily oriented spinning axis of the electric field might be observed. This includes the special case of a spinning axis perpendicular to the optical axis [18], which indicates the presence of purely transverse spin angular momentum (tSAM) [24,25]. While the rising interest in this intriguing polarization component is strongly linked to its occurrence in highly confined fields within guided modes and plasmons [26–28], it was shown that tSAM is also naturally present in many focusing scenarios [6,24,29–31]. As an example, even a linearly polarized fundamental Gaussian beam exhibits transversely spinning fields when tightly focused [6,31,32]. In this case, the transverse ($\mathbf{E}_\perp$) and longitudinal (E_z) electric field components exhibit in the focal plane a $\pi/2$ phase difference with respect to each other, and positions where both field components have the same amplitude represent *C* points that are linked to purely tSAM. This raises the question of whether those focal *C* points also exhibit complex polarization topologies.

In this Letter, we investigate the occurrence of Möbius-like optical polarization topologies in the focal field distribution of a tightly focused linearly polarized Gaussian beam. Furthermore, we show the generation of optical polarization Möbius strips around *C* points with nonzero transverse spin in the experimental realization of the mentioned field configuration using a nanointerferometric amplitude and phase reconstruction technique [20].

C points, transverse spin, and optical polarization Möbius strips.—When examining polarization topologies in fully vectorial and highly confined structured light fields, the electric field $\mathbf{E}$ at each point $\mathbf{r}$ is, in general, oscillating in a plane oriented arbitrarily in space. Thus, the local field can be described by a polarization ellipse with its major axis $\boldsymbol{\alpha}(\mathbf{r})$, minor axis $\boldsymbol{\beta}(\mathbf{r})$, and normal vector $\boldsymbol{\gamma}(\mathbf{r})$ defined in 3D space by [33]

$$\begin{aligned}\boldsymbol{\alpha} &= \frac{1}{|\sqrt{\mathbf{E}\cdot\mathbf{E}}|}\mathrm{Re}(\mathbf{E}^*\sqrt{\mathbf{E}\cdot\mathbf{E}}),\\ \boldsymbol{\beta} &= \frac{1}{|\sqrt{\mathbf{E}\cdot\mathbf{E}}|}\mathrm{Im}(\mathbf{E}^*\sqrt{\mathbf{E}\cdot\mathbf{E}}),\\ \boldsymbol{\gamma} &= \mathrm{Im}(\mathbf{E}^*\times\mathbf{E}),\end{aligned} \tag{1}$$

respectively, with $\mathbf{E}^*$ denoting the complex conjugate of the field. The field is oscillating in the plane spanned by $\boldsymbol{\alpha}$ and $\boldsymbol{\beta}$. The normal vector $\boldsymbol{\gamma}$ is, in this definition, directly proportional to the electric part of the spin density [34–36]:

$$\mathbf{s}_E(x,y,z) = \frac{\epsilon_0}{4\omega}\,\mathrm{Im}(\mathbf{E}^* \times \mathbf{E}), \tag{2}$$

with ϵ_0 the permittivity of free space and ω the angular frequency of the monochromatic light field. Since the electric spin density specifies the orientation and sense of the spinning axis of the local electric field and represents a physically measurable quantity [31,35], an elegant and straightforward method to determine points or lines of arbitrarily oriented circular polarization (C points or lines) or lines of arbitrarily oriented linear polarization (L lines) in a vectorial light field is to normalize $\mathbf{s}_E$ with the time-averaged energy density of the electric field, $w_E = (\epsilon_0/4)(|E_x|^2 + |E_y|^2 + |E_z|^2)$ [34]. This amplitude-independent measure is maximized when the polarization ellipse degenerates to a circle and zero when the ellipse degenerates to a line. We thus can define a simple requirement for C points:

$$\frac{|\mathbf{s}_E|}{w_E} = \frac{1}{\omega}. \tag{3}$$

As discussed before, the polarization ellipse can show intriguing topological patterns around such points in space, where we restrict ourselves in the following to C points. By choosing a plane of observation containing the C point and with the normal vector of that plane parallel to the spinning axis $\boldsymbol{\gamma}$ of the electric field at this C point, fundamental polarization topologies with a topological index of $\pm 1/2$ can be revealed [18,37]. This half integer index is allowed, since the orientation of a (polarization) ellipse is indistinguishable under a rotation by π [15].

Within the aforementioned formalism, we investigate the field distribution of a tightly focused y-polarized Gaussian beam propagating along z. This scenario corresponds to one of the most fundamental beam configurations in optics labs. Figure 1(a) depicts the electric energy density and phase (insets) distributions of all three Cartesian components in the focal plane [32,38] for a numerical aperture (NA) of 0.9, a wavelength of $\lambda = 530$ nm, and a fill factor of the focusing aperture of $w_0/f = 1.21$. The dominant field component $|E_y|^2$ has its maximum on the optical axis, while the longitudinal field $|E_z|^2$ shows a two-lobe structure, elongating the focal spot along the y axis [32,39]. The crossed polarization component $|E_x|^2$, occurring analog to the longitudinal field component due to a rotation of the polarization components upon focusing, exhibits the characteristic four-lobe structure observed in cross-polarization measurements [40] and referred to as depolarization [41]. Considering the relative phases between the field components, we see that the longitudinal component is $\pm\pi/2$ out of phase with respect to the in-phase transverse components, indicating purely transversely spinning fields throughout the focal plane. This can also be seen in the components of the electric spin density [see Fig. 1(b) and Ref. [31]] and is a feature exhibited by many fundamental beams after tight focusing. The strongest and, therefore, dominant component of the electric spin density is s_E^x. As expected, the longitudinal component s_E^z is identical zero, which implies that points of circular polarization in this case can be linked only to tSAM. In order to determine those C points of purely transverse spin, the ratio $|\mathbf{s}_E|/w_E$ is

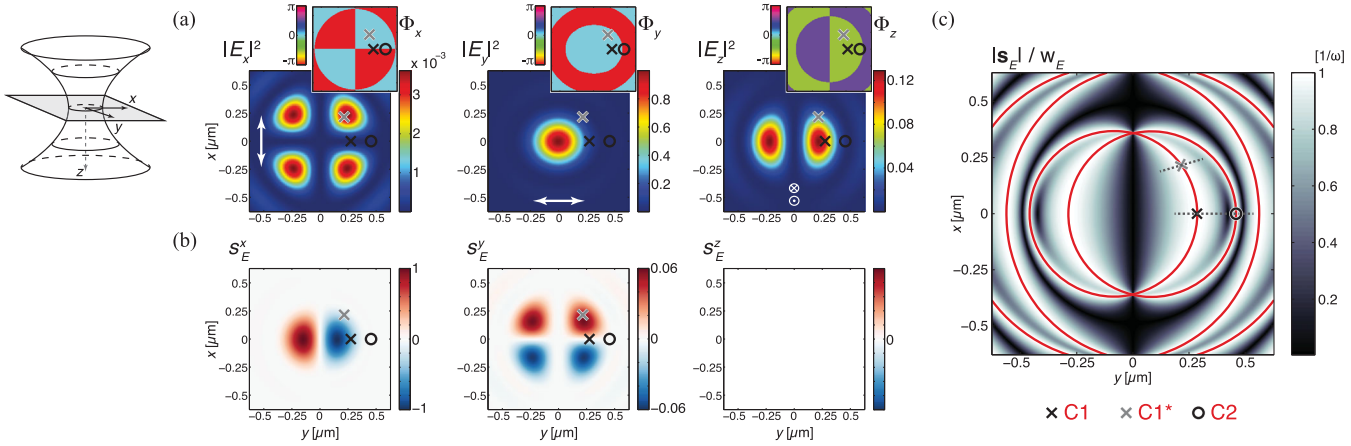

FIG. 1. (a) Theoretically calculated components of the focal electric energy density distribution $|E_x|^2$, $|E_y|^2$, and $|E_z|^2$ of a tightly focused linearly y-polarized Gaussian beam, normalized to the maximum electric energy density. Corresponding phase distributions are plotted as insets. (b) Distributions of the two nonzero components of the transverse spin density s_E^x and s_E^y in the focal plane (normalized to the maximum value of s_E^x). Because of the symmetry of the light field, s_E^z is identical zero across the whole focal plane. (c) Focal distribution of $|\mathbf{s}_E|$ normalized to the local electric energy density w_E. The red solid lines correspond to the maximum value $(1/\omega)$. The black and gray markers in all distributions correspond to the considered C points $C1$ and $C2$ on the y axis and $C1^*$ on the bisector of the positive x and y axis, while the gray dashed lines show the principal plane of their polarization circle.

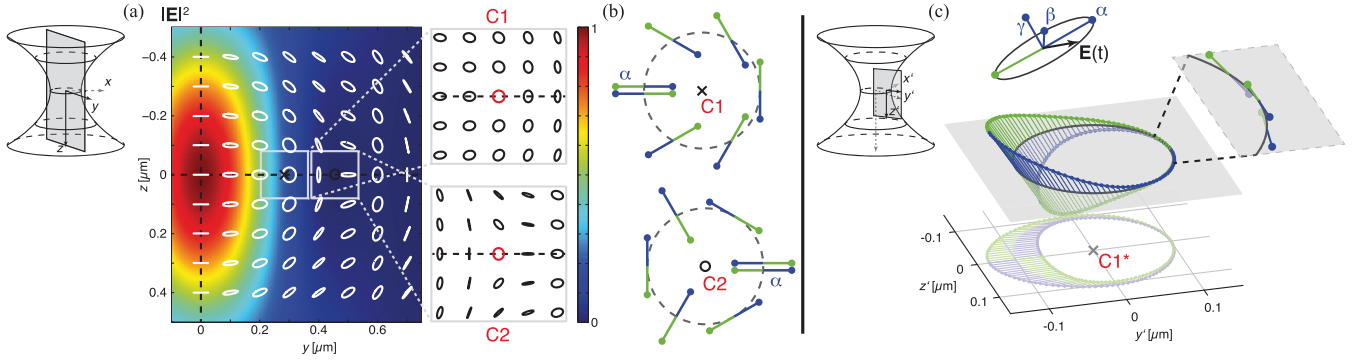

FIG. 2. (a) Electric energy density distribution in the yz plane, superimposed by the local polarization ellipses in white. Details in the vicinity of the first two C points $C1$ and $C2$ along the y axis are shown as insets. (b) Trace of the major axis of the polarization ellipse around the C points marked in red in the insets in (a). (c) Arising optical polarization topology when tracing around $C1^*$ (in the principal plane of its polarization ellipse with local coordinates x', y', $z' = z$) with a trace radius of 100 nm. The occurring weak x' component of the electric field is magnified 4 times to show the orientation of the major axis of the polarization ellipse more distinctly. The magnified part of the trace shows the major axis rotating into the principal plane and pointing along the trace direction.

plotted in Fig. 1(c). The red solid lines mark the C lines or, equivalently, lines along which Eq. (3) is fulfilled. In this theoretically calculated field distribution, C points can be found only in the actual focal plane of the linearly polarized tightly focused Gaussian beam. This is shown in Fig. 2(a), where the polarization ellipses are plotted as solid white lines on a cross section of the electric energy density in the yz plane containing the optical axis (meaning $x = 0$). Because of the different phase velocities for the transverse and longitudinal electric field components of the tightly focused beam, all polarization ellipses outside the focal plane form ellipses, which in the far field ($z \gg \lambda$) have to transform to the initially linear polarization.

In the following, we concentrate on three specific C points on two different C lines and investigate their polarization topologies in appropriately selected planes of observation. First, we examine a C point on the y axis, approximately 275 nm away from the optical axis ($C1$; see black crosses in Figs. 1 and 2), and look at the polarization ellipses in its principal plane (here, the yz plane). All electric field vectors and, therefore, also the polarization ellipses in this plane are in plane only, since $E_x(0, y, z) = 0$ [see also Fig. 1(a)]. Thus, we can use 2D polarization topologies to characterize the points of circular polarization in the chosen meridional plane of observation. With the terminology developed in Refs. [18,37,42], $C1$ represents a lemon-type polarization topology. The major axis of the polarization ellipse rotates clockwise when traced clockwise around the central C point and performs a rotation of π [see the upper part of Fig. 2(b)]. Thus, the topological index of $C1$ is $+1/2$. In contrast, the next C point on the y axis at a distance of approximately 455 nm ($C2$; see the black circle in Figs. 1 and 2) shows a star-type polarization topology [see the lower part of Fig. 2(b)], associated with an index of $-1/2$. This alternation of the two different planar topologies continues when moving further away from the optical axis.

The general structure of the occurring polarization topology and its local electric fields is limited to the yz plane due to the missing out-of-plane electric field component. This means that no 3D topologies can be observed in the yz plane, which is the plane of symmetry of the overall focusing geometry. However, the symmetry can be broken by investigating a C point off the y axis and choosing the principal plane of its polarization ellipse as the plane of observation. Along a C line, the topological index of the polarization singularity is conserved as long as the plane of observation (here chosen as the plane of the polarization ellipse) is not tangent to the C line [18]. Since this holds true for the chosen field configuration at all points except for the crossing point of both C lines where the electric field is identical zero, we examine exemplarily the C point on the bisector of the positive x and y axis closest to the optical axis ($C1^*$). Observing the field structure around this point in the coordinates x', y', z' (with $z' = z$) of its principal plane marked with a gray dashed line in Fig. 1(c), the electric field in the surrounding of the C point exhibits a 3D field configuration due to a nonzero $E_{x'}$ component; see also Fig. 1(a). This 3D field causes the major axis of the polarization ellipses around the C point to tilt out of plane. As a result, the previously two-dimensional ellipse field around $C1$ is transformed into a 3D structure around $C1^*$ with a topology similar to an optical polarization Möbius strip [see Fig. 2(c)]. To highlight the out-of-plane orientation of the polarization ellipses, the x' components of the plotted major axes are magnified by a factor of 4. The position of the discontinuity present in the trace of the major polarization axis is given by an arbitrary choice of the offset phase of the field [as in the planar case, also seen in the projection onto the $y'z'$ plane in Fig. 2(c)]. It is important to mention again that all components of the electromagnetic field are fully continuous at this point; only the major axis of the polarization ellipse exhibits a discontinuity. In contrast to the optical polarization Möbius strips investigated in Refs. [14–16], the major axis of the

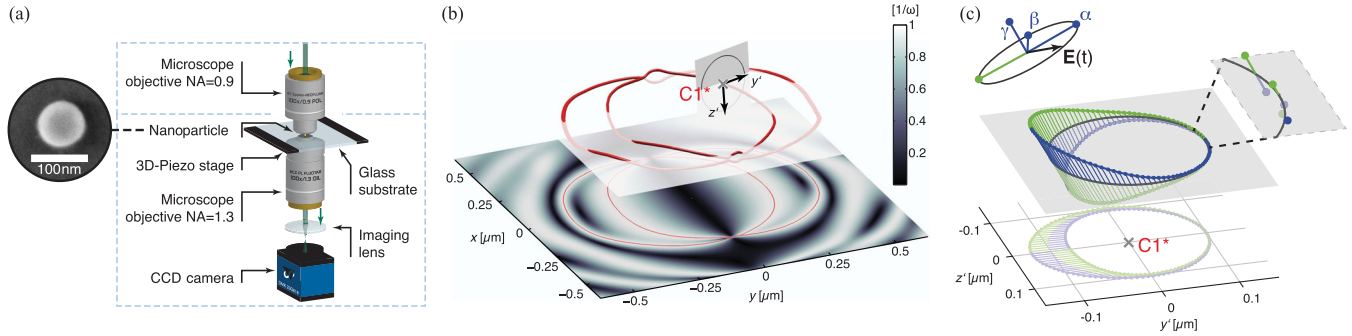

FIG. 3. (a) Sketch of the experimental setup for reconstructing highly confined field distributions. A SEM image of the employed gold nanoprobe is shown as an inset. (b) Experimentally reconstructed focal distribution of $|\mathbf{s}_E|/w_E$ with the two innermost C lines. The lower part depicts the projection of these C lines onto the focal plane and the corresponding distribution of $|\mathbf{s}_E|/w_E$. The red lines in the upper part of (b) depict the 3D trajectories of both C lines, which are crossing the focal plane (transparent white plane) repeatedly. The marked C point $C1^*$ corresponds to the one considered in (c). (c) Optical polarization Möbius strip with one half-twist, generated by tracing the major axis of the polarization ellipse around the C point on the bisector of the positive x and y axis in the plane normal to its local spin vector, marked in gray. The trace radius was chosen to be 100 nm. The magnified part of the trace shows that the major axis is, due to slight phase aberrations, not at the same time parallel to the principal plane and pointing along the trace direction. The occurring weak x' component of the electric field is magnified 4 times to show the half-twist of the major axis of the polarization ellipse more distinctly.

polarization ellipse is tangential to the chosen trace at one point [for $C1^*$, $z' = 0$ and $y' = 0.1$ μm; see the magnified part of Fig. 2(c)] due to the purely tSAM in the whole focal plane. This special orientation prevents the determination of the handedness and index of the twist of the major polarization axis when traced around the C point, rendering this case different from a generic Möbius strip. This indeterminacy holds true for all C points in this ideal field. However, as will be shown later on, only slight aberrations in the focal field distribution, for example, due to experimentally unavoidable phase aberrations, might lead to a distribution exhibiting not only purely tSAM. This implies that the major axis of the polarization ellipse is not tangential to the trace anymore, and, even at points with locally purely tSAM, the slight aberrations of the focal field will lead to a Möbius topology.

Experimental approach and results.—To verify this theoretical prediction, the experimental setup sketched in Fig. 3(a) [43] was used. The incoming linearly y-polarized Gaussian beam is tightly focused by a first microscope objective (MO) with a NA of 0.9. A spherical gold nanoparticle (radius $r = 42$ nm) on a glass substrate, acting as a local nanoprobe, is scanned through the focal plane. A second MO (immersion type, NA = 1.3) collects the transmitted field, including the light scattered off the particle in the forward direction. For each position of the nanoprobe relative to the optical axis, back-focal-plane images of the second MO are acquired, corresponding to the angular spectrum transmitted into the forward direction. These experimental data can be used to reconstruct the full vectorial focal field distribution following the technique introduced in Ref. [20], since amplitude and phase information are encoded in the angular interference between the transmitted beam and the scattered light. More details can be found in Supplemental Material [44].

Figure 3(b) illustrates the experimentally achieved distribution of $|\mathbf{s}_E|/w_E$, calculated from the reconstructed fully vectorial electric field distribution. Because of small experimental deviations from the theoretically expected field distribution, the experimentally reconstructed C lines not only are located in the focal plane but cross it repeatedly. These deviations can be explained by small aberrations of the incoming beam and the microscope objective. Tracing the major axis of the polarization ellipse around the C point at the same bisector used in Fig. 2(c) (gray crosses in Fig. 1) in the principal plane of its polarization ellipse results in the optical polarization Möbius strip with one half-twist as depicted in Fig. 3(c). This C point is not a point of purely tSAM in the experimental case due to the experimental aberrations and, thus, leads to the shown Möbius strip in agreement with the theoretical predictions. Also here, the out-of-plane component of the field was magnified by a factor of 4 to highlight the twist that can be seen in the magnified inset in Fig. 3(c). To confirm that also C points with purely tSAM exhibit these polarization topologies, the major axis of the polarization ellipse was additionally traced around such a C point (see Supplemental Material [44]). This demonstration of an optical polarization Möbius strip confirms the occurrence of this topological structure even in the basic scenario of a tightly focused linearly polarized beam.

Conclusion.—We investigated optical polarization topologies in a tightly focused linearly polarized Gaussian beam and showed that a special case of a Möbius-like topology, directly linked to the purely transverse spin density of the light field and the associated C lines in the focal plane, can be observed. By defining an appropriate plane of observation, we were able to trace the existing polarization topology around a C point with purely transverse spin. This

Möbius-like topology is present in an ideal beam at all C points located off the beam's symmetry axes. As experimental verification of the realized polarization topologies, we applied an interferometric nanoprobing technique, where slight aberrations of the focal field lead to the observation of generic optical polarization Möbius strips.

Our results demonstrate that even fundamental optical fields such as linearly polarized Gaussian beams can exhibit complex 3D polarization topologies under (tight) focusing conditions.

We gratefully acknowledge fruitful discussions with Mark R. Dennis and Ebrahim Karimi.

*peter.banzer@mpl.mpg.de; http://www.mpl.mpg.de/

[1] S. Quabis, R. Dorn, M. Eberler, O. Glöckl, and G. Leuchs, Focusing light to a tighter spot, Opt. Commun. **179**, 1 (2000).
[2] K. Youngworth and T. Brown, Focusing of high numerical aperture cylindrical-vector beams, Opt. Express **7**, 77 (2000).
[3] E. Rittweger, K. Y. Han, S. E. Irvine, C. Eggeling, and S. W. Hell, STED microscopy reveals crystal colour centres with nanometric resolution, Nature Photon. **3**, 144 (2009).
[4] T. Züchner, A. V. Failla, A. Hartschuh, and A. J. Meixner, A novel approach to detect and characterize the scattering patterns of single Au nanoparticles using confocal microscopy, J. Microsc. **229**, 337 (2008).
[5] J. Sancho-Parramon and S. Bosch, Dark modes and Fano resonances in plasmonic clusters excited by cylindrical vector beams, ACS Nano **6**, 8415 (2012).
[6] M. Neugebauer, T. Bauer, P. Banzer, and G. Leuchs, Polarization tailored light driven directional optical nanobeacon, Nano Lett. **14**, 2546 (2014).
[7] P. Woźniak, P. Banzer, and G. Leuchs, Selective switching of individual multipole resonances in single dielectric nanoparticles, Laser Photonics Rev. **9**, 231 (2015).
[8] K. Dholakia and T. Čižmár, Shaping the future of manipulation, Nature Photon. **5**, 335 (2011).
[9] M. A. Taylor, M. Waleed, A. B. Stilgoe, H. Rubinsztein-Dunlop, and W. P. Bowen, Enhanced optical trapping via structured scattering, Nature Photon. **9**, 669 (2015).
[10] J. F. Nye and M. V. Berry, Dislocations in wave trains, Proc. R. Soc. A **336**, 165 (1974).
[11] L. Allen, M. W. Beijersbergen, R. J. C. Spreeuw, and J. P. Woerdman, Orbital angular momentum of light and the transformation of Laguerre-Gaussian laser modes, Phys. Rev. A **45**, 8185 (1992).
[12] J. Leach, M. R. Dennis, J. Courtial, and M. J. Padgett, Knotted threads of darkness, Nature (London) **432**, 165 (2004).
[13] M. R. Dennis, R. P. King, B. Jack, K. O'Holleran, and M. J. Padgett, Isolated optical vortex knots, Nat. Phys. **6**, 118 (2010).
[14] I. Freund, Cones, spirals, and Möbius strips, in elliptically polarized light, Opt. Commun. **249**, 7 (2005).
[15] M. R. Dennis, Fermionic out-of-plane structure of polarization singularities, Opt. Lett. **36**, 3765 (2011).
[16] T. Bauer, P. Banzer, E. Karimi, S. Orlov, A. Rubano, L. Marrucci, E. Santamato, R. W. Boyd, and G. Leuchs, Observation of optical polarization Möbius strips, Science **347**, 964 (2015).
[17] A. Garcia-Etxarri, Polarization singularities on high index nanoparticles, arXiv:1601.04365.
[18] J. F. Nye and J. V. Hajnal, The wave structure of monochromatic electromagnetic radiation, Proc. R. Soc. A **409**, 21 (1987).
[19] I. Freund, Multitwist optical Möbius strips, Opt. Lett. **35**, 148 (2010).
[20] T. Bauer, S. Orlov, U. Peschel, P. Banzer, and G. Leuchs, Nanointerferometric amplitude and phase reconstruction of tightly focused vector beams, Nature Photon. **8**, 23 (2014).
[21] A. M. Beckley, T. G. Brown, and M. A. Alonso, Full Poincaré beams, Opt. Express **18**, 10777 (2010).
[22] E. J. Galvez, S. Khadka, W. H. Schubert, and S. Nomoto, Poincaré-beam patterns produced by nonseparable superpositions of Laguerre-Gauss and polarization modes of light, Appl. Opt. **51**, 2925 (2012).
[23] F. Cardano, E. Karimi, L. Marrucci, C. de Lisio, and E. Santamato, Generation and dynamics of optical beams with polarization singularities, Opt. Express **21**, 8815 (2013).
[24] A. Aiello, P. Banzer, M. Neugebauer, and G. Leuchs, From transverse angular momentum to photonic wheels, Nature Photon. **9**, 789 (2015).
[25] K. Y. Bliokh and F. Nori, Transverse and longitudinal angular momenta of light, Phys. Rep. **592**, 1 (2015).
[26] K. Y. Bliokh and F. Nori, Transverse spin of a surface polariton, Phys. Rev. A **85**, 061801 (2012).
[27] F. J. Rodríguez-Fortuño, G. Marino, P. Ginzburg, D. O'Connor, A. Martínez, G. A. Wurtz, and A. V. Zayats, Near-field interference for the unidirectional excitation of electromagnetic guided modes, Science **340**, 328 (2013).
[28] J. Petersen, J. Volz, and A. Rauschenbeutel, Chiral nanophotonic waveguide interface based on spin-orbit interaction of light, Science **346**, 67 (2014).
[29] N. Yang and A. E. Cohen, Local geometry of electromagnetic fields and its role in molecular multipole transitions, J. Phys. Chem. B **115**, 5304 (2011).
[30] P. Banzer, M. Neugebauer, A. Aiello, C. Marquardt, N. Lindlein, T. Bauer, and G. Leuchs, The photonic wheel—demonstration of a state of light with purely transverse angular momentum, J. Eur. Opt. Soc. **8**, 13032 (2013).
[31] M. Neugebauer, T. Bauer, A. Aiello, and P. Banzer, Measuring the Transverse Spin Density of Light, Phys. Rev. Lett. **114**, 063901 (2015).
[32] B. Richards and E. Wolf, Electromagnetic diffraction in optical systems. II. Structure of the image field in an aplanatic system, Proc. R. Soc. A **253**, 358 (1959).
[33] M. V. Berry, Index formulae for singular lines of polarization, J. Opt. A **6**, 675 (2004).
[34] M. V. Berry and M. R. Dennis, Polarization singularities in isotropic random vector waves, Proc. R. Soc. A **457**, 141 (2001).
[35] K. Y. Bliokh, A. Y. Bekshaev, and F. Nori, Extraordinary momentum and spin in evanescent waves, Nat. Commun. **5**, 3300 (2014).
[36] A. Aiello and P. Banzer, Transverse spin of light for all wavefields, arXiv:1502.05350.

[37] M. V. Berry and J. H. Hannay, Umbilic points on Gaussian random surfaces, J. Phys. A **10**, 1809 (1977).
[38] L. Novotny and B. Hecht, *Principles of Nano-Optics* (Cambridge University Press, Cambridge, England, 2006).
[39] R. Dorn, S. Quabis, and G. Leuchs, The focus of light—linear polarization breaks the rotational symmetry of the focal spot, J. Mod. Opt. **50**, 1917 (2003).
[40] L. Novotny, R. D. Grober, and K. Karrai, Reflected image of a strongly focused spot, Opt. Lett. **26**, 789 (2001).
[41] K. Bahlmann and S. W. Hell, Depolarization by high aperture focusing, Appl. Phys. Lett. **77**, 612 (2000).
[42] M. R. Dennis, Polarization singularities in paraxial vector fields: Morphology and statistics, Opt. Commun. **213**, 201 (2002).
[43] P. Banzer, U. Peschel, S. Quabis, and G. Leuchs, On the experimental investigation of the electric and magnetic response of a single nano-structure, Opt. Express **18**, 10905 (2010).
[44] See Supplemental Material at http://link.aps.org/supplemental/10.1103/PhysRevLett.117.013601 for details about the experimentally measured interferometric data and reconstructed focal field distribution.